POLARIZATION OF CONTINUUM RADIATION IN MAGNETIC ATMOSPHERES

K. N. NAGENDRA and A. PERAIAH
Indian Institute of Astrophysics, Bangalore, India

(Received 16 January, 1984)

Abstract. A numerical solution is presented for the problem of continuum radiative transfer in a magneto-active medium. The continuum opacities are calculated in the presence of a strong magnetic field ($H = 10^7$ G) typical of magnetic white dwarfs. The L.T.E. pure absorption model is assumed for calculating the polarized radiation field emitted by a realistic model atmosphere in the plane parallel approximation. The wavelength dependence of the linear and circular polarizations are calculated for both uniform and dipole field configurations.

1. Introduction

It is well known that some of the white dwarfs are magnetic. The continuum radiation emitted by these stars is polarized because of the presence of strong magnetic fields ($H > 10^7$ G) in their atmospheres. The observed linear and circular polarizations of these strong field white dwarfs show a wavelength dependence. (See the review article by Angel (1978) for a detailed discussion on magnetic white dwarfs.) Shipman (1971) calculated the polarization spectra using an analytic treatment of radiative transfer. His approach was later extended by Angel and Landstreet (1974). The transfer equations for magnetic polarization was also solved in the so-called 'normal wave representation' by Gnedin and Pavlov (1974). In a recent series of papers, Martin and Wickramasinghe (1978, 1979a, b, 1981, 1982) have carried out more accurate calculations of flux and polarization using realistic model atmospheres and field geometries. In the preliminary calculations presented in this paper we have solved numerically the vector transfer equation for the polarized light.

2. Calculation of Dichroic Opacities

The important sources of continuous opacity in cool white dwarfs are the bound-free and free-free transitions of H, H^-, He, and He^-. We have used a non-magnetic model atmosphere provided by Wehrse (private communication) with the following parameters: $T_e = 9000$ K, $\log g = 8.0$, $\log A(\mathrm{He})$ = solar value, $\log A(\mathrm{C, N, O})$ = solar value, and $\log A(\mathrm{metals})$ = solar value -2.0 (A = elemental abundance). We have computed all the non-magnetic opacities mentioned above using the polynomial approximations given in Kuruz (1970).

2.1. Bound-free dichroism

If we follow Lamb and Sutherland (1974), the field-free opacity (mass absorption

Astrophysics and Space Science **104** (1984) 61–72. 0004–640X/84/1041–0061$01.80.

coefficient) at a frequency ν can be given for hydrogen-like atoms by

$$k(\nu) = \text{const.}\ \nu f(\nu)\,, \tag{1}$$

where $f(\nu)$ is a continuous function of frequency ν. In an approximation introduced by the same authors, the opacities in the presence of a strong magnetic field for the right circularly polarized light (corresponding to a $\Delta M = +1$ transition) and left circularly polarized light (corresponding to a $\Delta M = -1$ transition) are given by

$$k_{\Delta M}(\nu) = \text{const.}\ \nu f(\nu - \Delta M \nu_L)\,,$$
$$\Delta M = M_f - M_i = 0\,,\ \pm 1\,, \qquad \nu_L = eH/4\pi mc\,, \tag{2}$$

where M_f and M_i are the final and initial state magnetic quantum numbers, respectively, and ν_L is the Larmor frequency. Equations (2) are accurate to first order in (ν_L/ν). From Equations (1) and (2), the magnetic dichroism is calculated by

$$\left(\frac{\Delta k}{k}\right)_\nu = \frac{k_+(\nu) - k_-(\nu)}{k_0(\nu)} = \frac{f(\nu - \nu_L) - f(\nu + \nu_L)}{f(\nu)}\,. \tag{3}$$

Expanding the functions $f(\nu - \nu_L)$ and $f(\nu + \nu_L)$ in a Taylor series about ν, one obtains correctly to $O((\nu_L/\nu)$,

$$\left(\frac{\Delta k}{k}\right)_\nu = -2\nu_L \frac{\mathrm{d}f(\nu)}{\mathrm{d}\nu}\,. \tag{4}$$

If $k_0(\nu) = \text{const.}\ \nu^{-\alpha}$, where α = spectral index of opacity, then from Equations (1) and (4) we get

$$\left(\frac{\Delta k}{k}\right)_\nu = 2(\alpha + 1)\frac{\nu_L}{\nu}\,. \tag{5}$$

Equation (5) is very useful for an approximate calculation of circular dichroism. The coefficients $k_+(\nu)$ and $k_-(\nu)$ can be calculated separately in the following manner. From Equation (1) we get (under the rigid wave function approximation of Lamb and Sutherland)

$$f(\nu - \nu_L) = \frac{k_0(\nu - \nu_L)}{\text{const.}\,(\nu - \nu_L)}\,, \tag{6a}$$

$$f(\nu + \nu_L) = \frac{k_0(\nu + \nu_L)}{\text{const.}\,(\nu + \nu_L)}\,, \tag{6b}$$

$$f(\nu) = \frac{k_0(\nu)}{\text{const.}\ \nu}\,; \tag{6c}$$

and substituting Equations (6a) and (6b) in Equation (2), we find that

$$k_+(\nu) = \frac{\nu}{(\nu - \nu_L)} k_0(\nu - \nu_L), \tag{7a}$$

$$k_-(\nu) = \frac{\nu}{(\nu + \nu_L)} k_0(\nu + \nu_L). \tag{7b}$$

It can be verified that this approximation gives the same result as expressed in Equation (4). Substituting Equations (6a, b, c) into Equation (3), and after simple algebra one gets for an opacity varying like $k_0(\nu) = \text{const.}\ \nu^{-\alpha}$, the general expression

$$\left(\frac{\Delta k}{k}\right)_\nu = \nu \left[\frac{2(\alpha + 1)\nu^\alpha \nu_L + 2(\alpha - 1)\nu\, \nu_L^\alpha}{\nu^{-\alpha}(\nu + \nu_L)^{\alpha+1}(\nu - \nu_L)^{\alpha+1}}\right]. \tag{8}$$

For $\nu_L \ll \nu$, which is satisfied for weaker fields, Equation (8) reduces to Equation (4) as

$$\left(\frac{\Delta k}{k}\right)_\nu = \nu \left[\frac{2(\alpha + 1)\nu^\alpha \nu_L}{\nu^{-\alpha}\nu^{2(\alpha+1)}}\right] = 2(\alpha + 1)\frac{\nu_L}{\nu}. \tag{9}$$

We have computed $k_+(\nu)$ and $k_-(\nu)$ from Equations (7a) and (7b) for $H = 10^7$ G, at all the depth points for the given frequency. The wavelength dependence of the dichroic opacities of H bound-free transitions is shown in Figure 1a. We have plotted the values of opacities at an optical depth $\tau_{5000} \sim 0.75$ where the local temperature $T \sim 9050$ K. The behaviour of the dichroism at the absorption edges predicted by Lamb and Sutherland (1974) is also shown. The strong polarization changes that occur at these edges can manifest themselves in the spectrum even after integrating over the stellar disk. Using the same prescription as above (Equations (7a) and (7b)) the H^- bound-free opacity is computed in Figure 1b. This opacity dominates in the optical wavelengths and reaches its maximum in the infrared. The opacity and dichroism of H^- ion bound-free transitions play a key role in producing the polarization spectra in the present model. We have included the He bound-free dichroism also in the calculation using the hydrogenic approximation (the same coefficient $\alpha = 3$ was used by Lamb and Sutherland for both H and He bound-free dichroism). But its contribution to the opacity and dichroism is much smaller in the present model.

2.2. Free-free dichroism

Free-free dichroism for H and He were predicted by Kemp (1977). The coefficient $\alpha \sim 3.0$ for both H and He atoms (Kemp, 1977). As a first approximation we have used the Lamb–Sutherland frequency shifts for the calculation of free-free dichroism also, Figure 2a. It can be seen from the figure that the contribution to dichroism is significant in the far infrared ($\lambda > 13\,000$ Å) though the opacity is still smaller, except in the deepest layers, for the present model. The contribution to total dichroism from He free-free transitions is again very small for the temperatures that we have considered. The H^- free-free dichroism ($\alpha \geq 1$) was first introduced through the method mentioned earlier

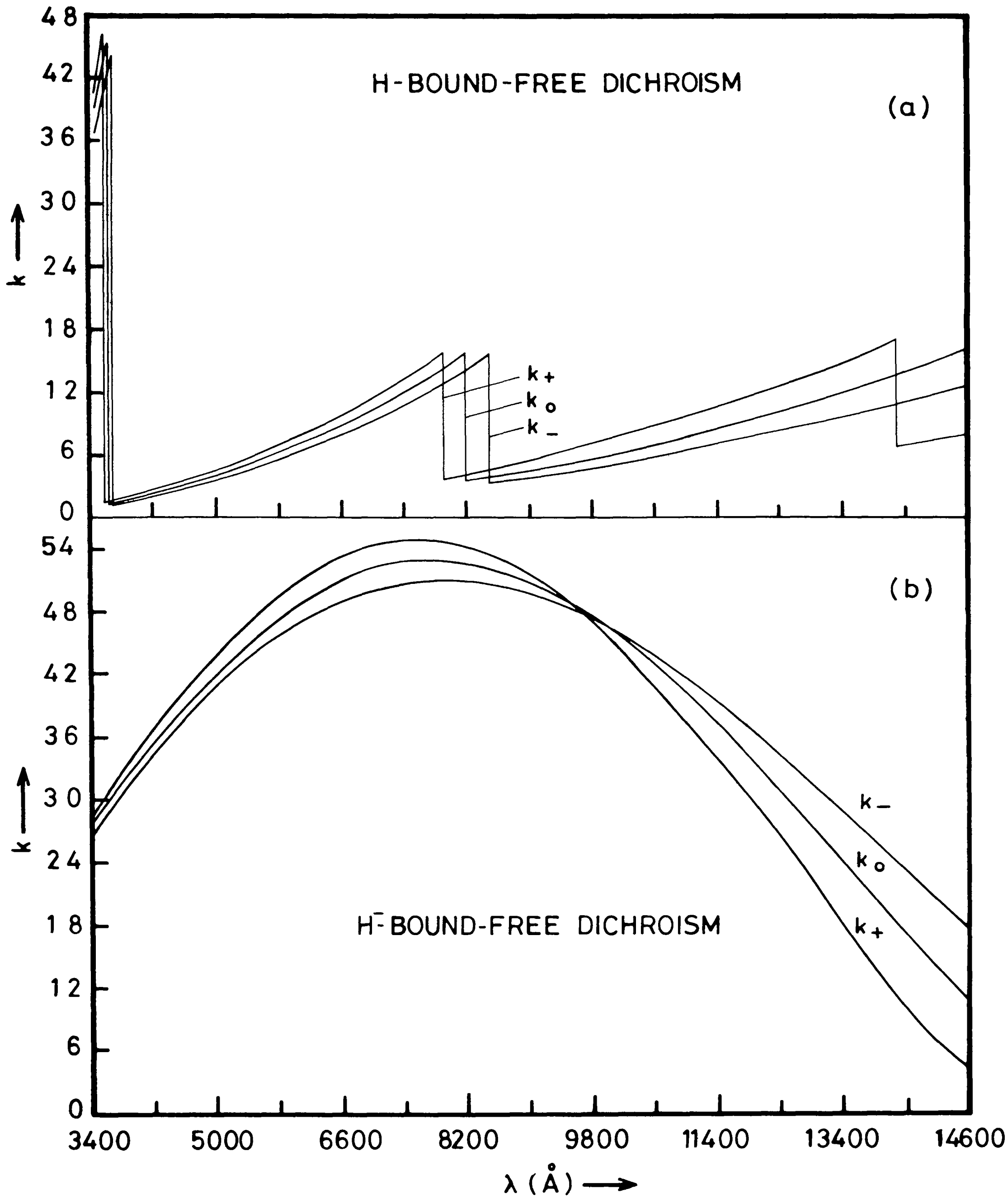

Fig. 1. Wavelength dependence of the dichroic opacities k_0, k_+, and k_- for $H = 10^7$ G. The symbol k represents the mass absorption coefficient (in the units g^{-1} cm^2). The values correspond to an optical depth $\tau(\lambda = 5000$ Å$) \sim 0.75$, where $T = 9040$ K. (a) Hydrogen bound-free dichroism. (b) Negative hydrogen ion (H^-) bound-free dichroism.

(Equation (4)) and used for comparison with observations by Liebert *et al.* (1975). In the model employed by us H^- free-free is an important source of dichroism and opacity particularly in the infrared, see Figure 2b. The H^- free-free dichroism (for which $\alpha \simeq 1.85$) is shown in Figure 2c. An extension of the rigid wave-function approximation

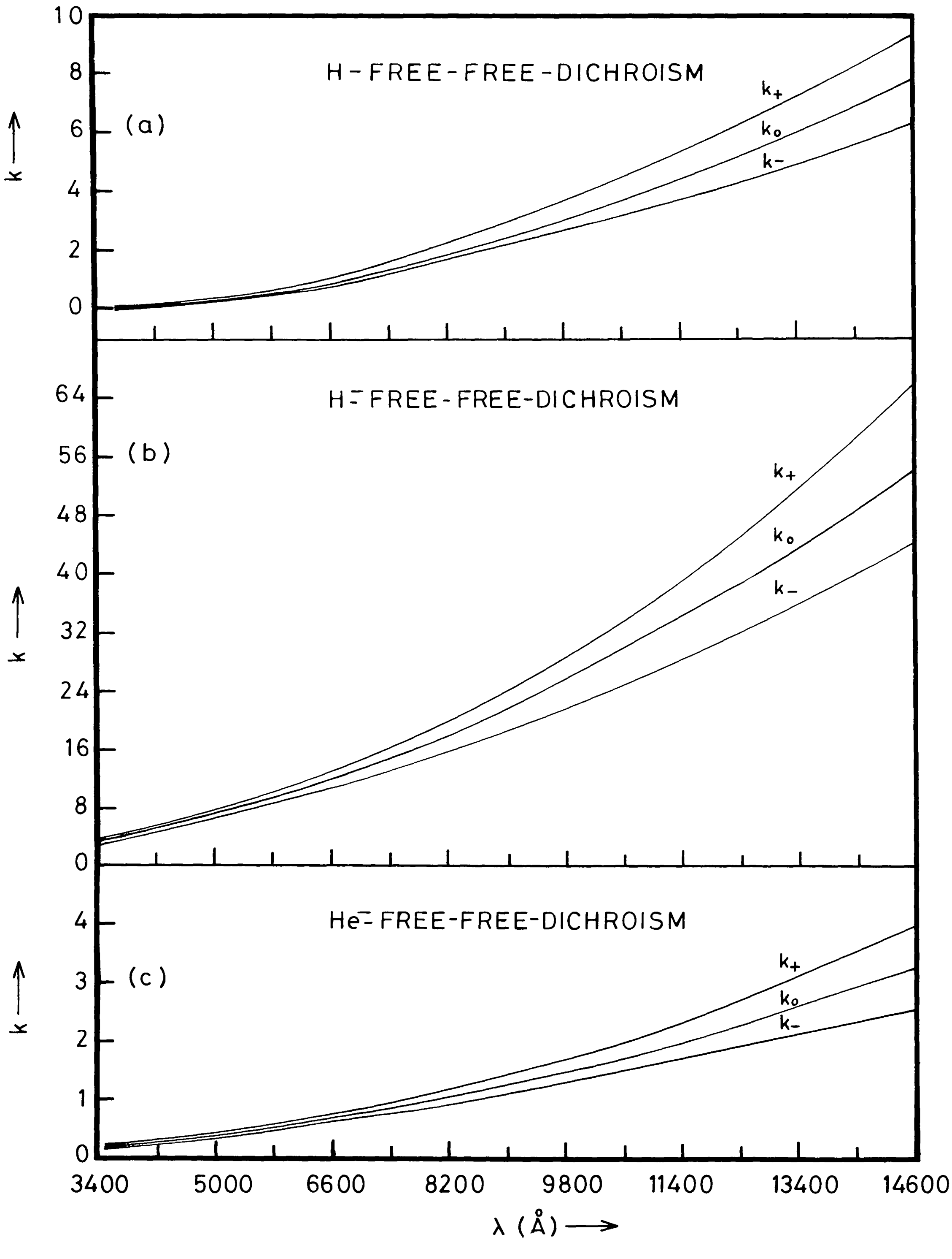

Fig. 2. Same as Figure 1 but for free-free dichroic opacities. (a) Hydrogen free-free dichroism. (b) Negative hydrogen ion dichroism. (c) Negative helium ion (He^-) dichroism.

to this important source of opacity in cooler He-rich stars was made by Landstreet and Angel (1975). Because of the lower abundance of helium, this source of opacity and dichroism has a smaller effect on the emergent polarization and flux. Figures 1a, b; 2a, b, c are intended to show the relative contribution to total opacity and dichroism by different absorbers. The main emphasis is to approximately indicate the regions of the spectrum where flux and polarization can be expected to undergo noticeable changes.

3. Equations of the Problem

The Unno transfer equations (Unno, 1956) for magneto-absorption including magnetic birefringence are given (see Martin and Wickramasinghe, 1979b) by

$$\mu \frac{\mathrm{d}I}{\mathrm{d}Z} = -(K_I I + K_Q Q + K_V V) + K_I B , \tag{1}$$

$$\mu \frac{\mathrm{d}Q}{\mathrm{d}Z} = -(K_Q I + K_I Q - \rho_R' U) + K_Q B , \tag{2}$$

$$\mu \frac{\mathrm{d}U}{\mathrm{d}Z} = -(\rho_R' Q + K_I U - \rho_W' V) , \tag{3}$$

$$\mu \frac{\mathrm{d}V}{\mathrm{d}Z} = -(K_V I + \rho_W' U + K_I V) + K_V B ; \tag{4}$$

where $I = (IQUV)^T$ is the Stokes vector with the four Stokes parameters as components. $\mu = \cos\theta$, θ = angle between the ray direction and the axis along which the optical depth is measured (Z-axis). B is the local source function which is just the Planck function in L.T.E. approximation. The absorption coefficients for the Stokes parameters are given by

$$K_I = \tfrac{1}{2}k_p' \sin^2\psi + \tfrac{1}{4}(k_l' + k_r')(1 + \cos^2\psi) , \tag{5}$$

$$K_Q = \tfrac{1}{2}k_p' \sin^2\psi - \tfrac{1}{4}(k_l' + k_r') \sin^2\psi , \tag{6}$$

$$K_V = \tfrac{1}{2}(k_r' - k_l') \cos\psi ; \tag{7}$$

where ψ is the angle between the direction of the ray and the direction of the magnetic field. k_p', k_l', and k_r' are the Zeeman-shifted continuous absorption coefficients. The solution $(IQUV)^T$ to Equations (1)–(4) is to be multiplied by

$$\begin{bmatrix} 1 & 0 & 0 & 0 \\ 0 & \cos 2\phi & -\sin 2\phi & 0 \\ 0 & \sin 2\phi & \cos 2\phi & 0 \\ 0 & 0 & 0 & 0 \end{bmatrix} \tag{8}$$

to obtain the actual solution for an arbitrary orientation of the magnetic field in a coordinate system in which ϕ is the field azimuth w.r.t. an arbitrary X-axis at right angles to the line-of-sight. The parameters ρ'_R and ρ'_W represent the magneto-optical effects due to free electrons. ρ'_R produces a rotation of the electric vector of linearly polarized light. ρ'_W leads to a phase retardation between the linear polarizations parallel and perpendicular to the field direction. These parameters for $\omega \gg \omega_c$ are given by

$$\rho'_R = -\frac{\omega_p^2 \omega_c \cos\psi}{c(\omega^2 - \omega_c^2)}, \tag{9}$$

$$\rho'_W = -\frac{\omega_p^2 \omega_c^2 \sin^2\psi}{2c\omega(\omega^2 - \omega_c^2)}; \tag{10}$$

where $\omega_p = (4\pi Ne^2/m)$ is the plasma frequency and $\omega_c = eH/mc$ is the cyclotron frequency. k'_p, k'_l, and k'_r are the continuous absorption coefficients at the Zeeman shifted frequencies when it is assumed that all the sources of opacities are dichroic ($k'_p = k_0$, $k'_l = k_-$, $k'_r = k_+$). We can also select only those opacities as dichroic for which Lamb–Sutherland shifts are known to be applicable (Landstreet and Angel, 1975). With this choice Equations (5)–(7) become

$$K_I = \beta + \tfrac{1}{2}k_p \sin^2\psi + \tfrac{1}{4}(k_l + k_r)(1 + \cos^2\psi), \tag{11}$$

$$K_Q = \tfrac{1}{2}k_p \sin^2\psi - \tfrac{1}{4}(k_l + k_r)\sin^2\psi, \tag{12}$$

$$K_V = \tfrac{1}{2}(k_r - k_l)\cos\psi; \tag{13}$$

where $\beta = (k^c - k_p)$ is the 'residual opacity'. $k_p = k_0$ (H–bf, H–ff, He–bf, He–ff, H^-–bf, h^-–ff, He^-–ff) is the 'selective' continuous opacity for p electrons in our choice (see Unno, 1956; p. 113). Defining an optical depth scale $d\tau = -k^c\rho\, dZ$ using the non-magnetic opacity k^c, we can write Equations (1)–(4) as

$$\mu \frac{dI}{d\tau} = \eta_I(I - B) + \eta_Q Q + \eta_V V, \tag{14}$$

$$\mu \frac{dQ}{d\tau} = \eta_Q(I - B) + \eta_I Q - \rho_R U, \tag{15}$$

$$\mu \frac{dU}{d\tau} = \rho_R Q + \eta_I U - \rho_W V, \tag{16}$$

$$\mu \frac{dV}{d\tau} = \eta_V(I - B) + \rho_W U + \eta_I V; \tag{17}$$

with

$$\eta_I = \left(\frac{K_I}{k^c}\right) = \varepsilon + \tfrac{1}{2}\eta_p \sin^2\psi + \tfrac{1}{4}(\eta_l + \eta_r)(1 + \cos^2\psi) \tag{18}$$

and

$$\eta_Q = (K_Q/k^c), \qquad \eta_V = (K_V/k^c), \qquad \eta_{p,l,r} = (k_{p,l,r}/k^c),$$

$$\rho_{R,W} = (\rho'_{R,W}/k^c) \quad \text{and} \quad \varepsilon = (\beta/k^c).$$

Note that $\varepsilon \ll 1$. Equations (14)–(17) represent outgoing rays ($0 < \mu \leq 1$). The same set of equations represents the inward going rays by replacing μ by $(-\mu)$, ($0 < \mu \leq 1$). The method of solution which is based on the 'discrete space theory of radiative transfer', Grant and Hunt (1968, 1969a, b) and Peraiah and Grant (1973) suitably modified for the case of magnetized media will be presented in another paper along with a detailed comparison with some standard methods of solution. The Unno solution for Equations (14)–(17) at $\tau = \tau_{max}$ can be employed as a suitable boundary condition for the problem, Martin and Wickramasinghe (1979b, p. 886) and Stenflo (1971).

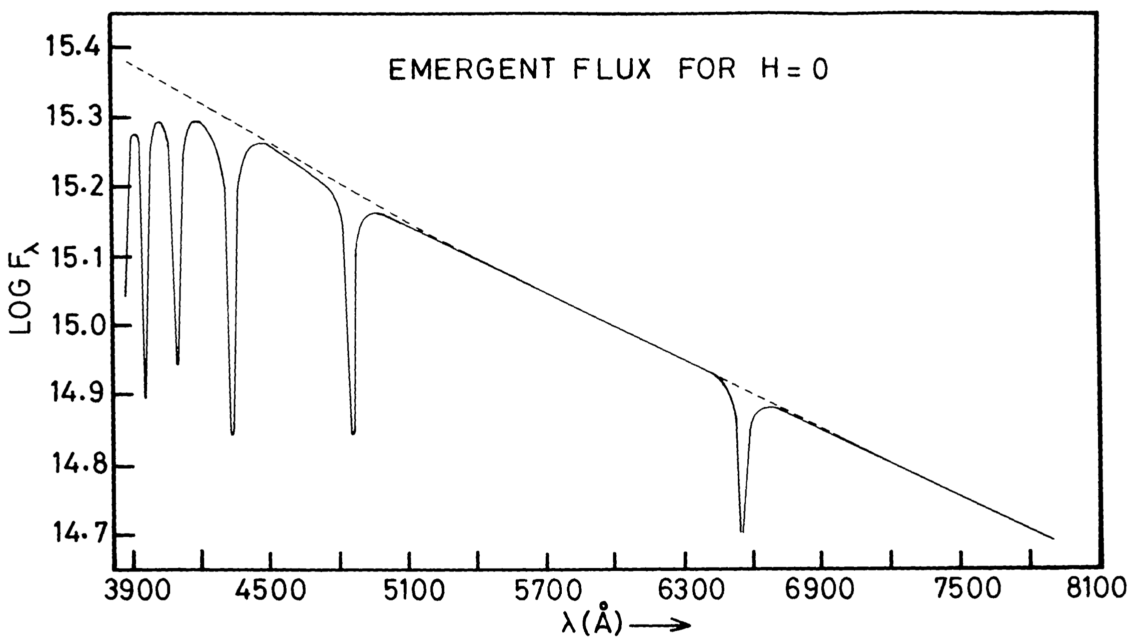

Fig. 3. Comparison of our zero-field ($H = 0$) emergent flux (dashed line) with line-blanketed flux taken from Wehrse (solid line). The flux units are erg cm^{-2} s^{-1} per unit wavelength interval $\Delta\lambda = 1$ cm.

4. Discussion and Conclusions

First we will discuss the results for a uniform magnetic field H ($= 10^7$ G) directed along the Z-axis. The medium is devided into 26 layers for the optical depth integration of the transfer equation. For convenience in the calculation of flux, we have solved the equations at the roots of a gaussian quadrature. In Figure 3 a comparison of the non-magnetic emergent fluxes

$$F_\lambda = F_I(\tau = 0) = 2\pi \int_0^1 I(0, \mu)\mu \, d\mu ,$$

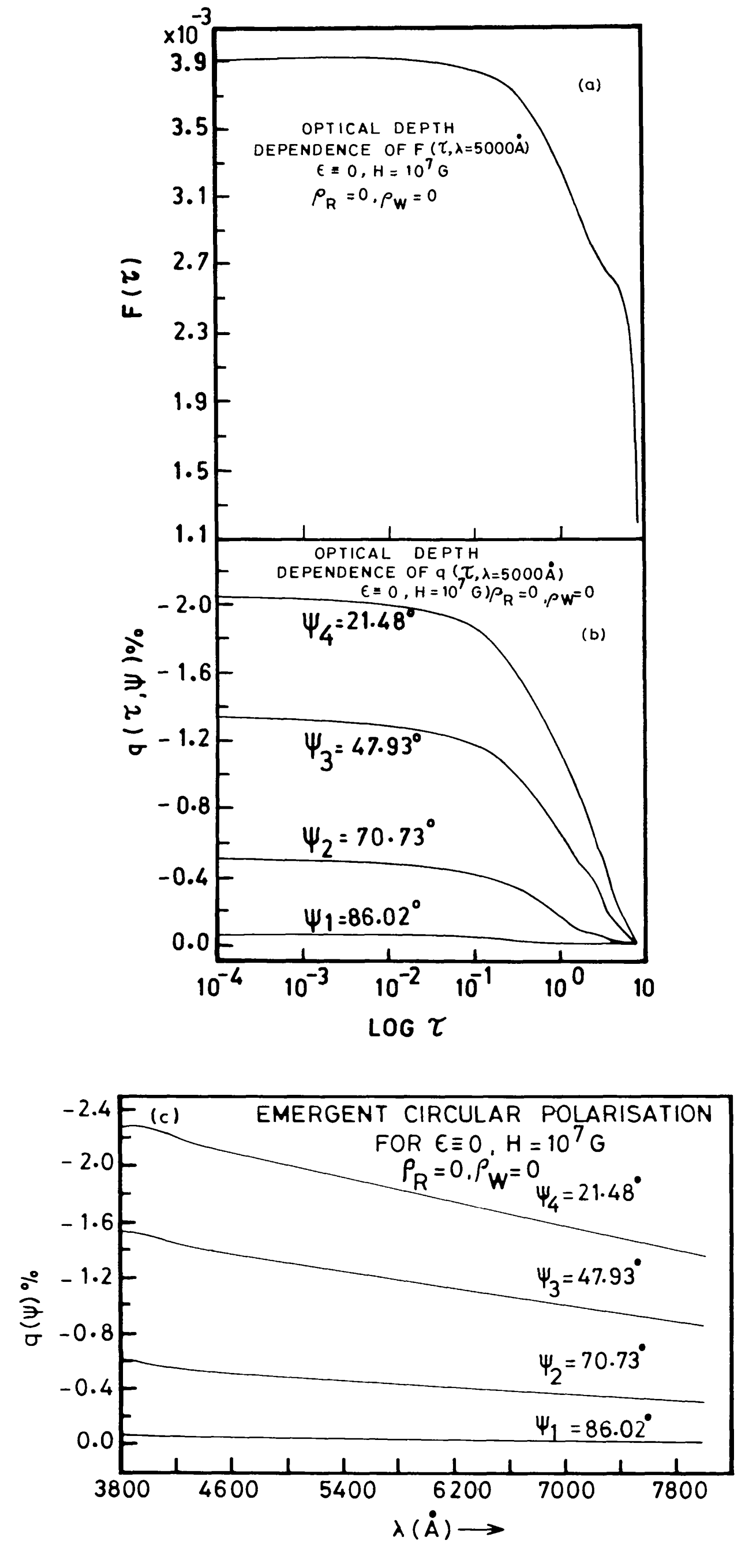

Fig. 4. Optical depth dependence of flux and circular polarization. (a) Net flux as a function of optical depth τ (λ = 5000 Å), in units of erg cm^{-2} s^{-1} Hz^{-1}. (b) Circular polarization (percentage) as a function of optical depth for $H = 10^7$ G. ψ is the angle between line-of-sight and magnetic field. (c) Wavelength dependence of circular polarization for different values of ψ.

($I(0, \mu)$ = Stokes I parameter) is made with the tabulated fluxes taken from Wehrse's model (1976). The net flux

$$F(\tau) = F_I(\tau) = 2\pi \int_{-1}^{+1} I(\tau, \mu)\mu \, d\mu$$

for $\lambda = 5000$ Å, Figure 4a increases from $\tau = 8.0$ to $\tau = 0.1$, after which it remains constant. The magnetic fluxes are slightly smaller than the non-magnetic fluxes. The

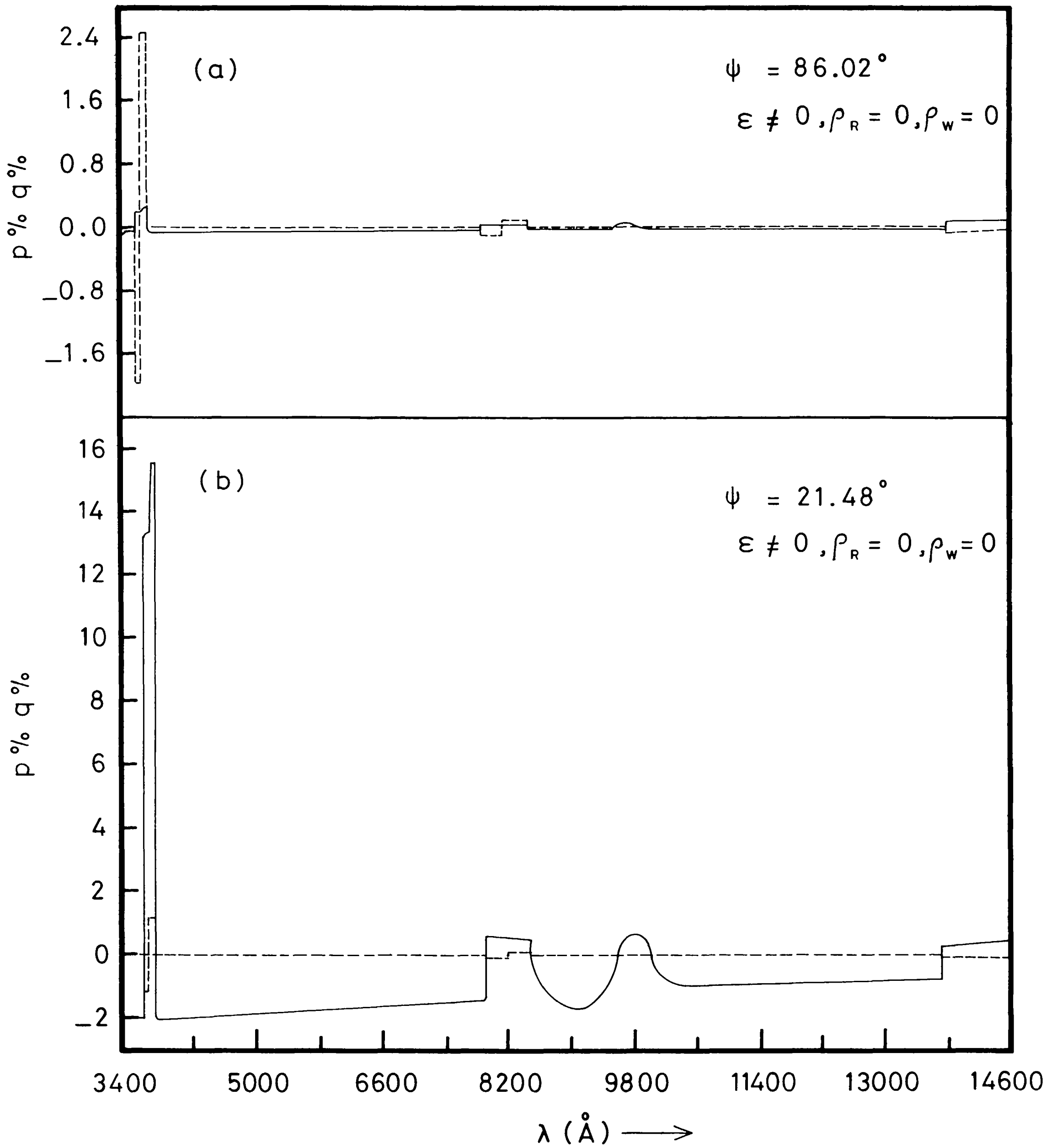

Fig. 5. Wavelength dependence of linear polarization P (dashed line) and circular polarization q (full line) for $H = 10^7$ G, and a selective absorption ($\varepsilon \neq 0$). (a) $\psi = 86.02°$. (b) $\psi = 21.48°$.

degree of circular polarization $q(\tau, \psi) = V(\tau, \psi)/I(\tau, \psi)$ assuming the entire opacity as dichroic ($\varepsilon \equiv 0$) is shown in Figure 4b. The polarization of a ray of light increases in an analogous manner to the net flux. The transfer effects are stronger in deeper layers ($\tau > 0.1$). The degree of circular polarization is larger for smaller values of the angle ψ, Figures 4a and c. This behavior is as expected for an absorbing layer of Zeeman-active gas. The wavelength dependence of q (Figure 4c) reflects the wavelength dependence of the flux unless there is a source function gradient reversal which for instance can arise as a result of a discontinuity in the opacity. The effect of such an absorption 'edge' on the linear polarization p ($= p(\psi) = Q(\psi)/I(\psi)$) and the circular polarization q ($= q(\psi) = V(\psi)/I(\psi)$) is shown in Figures 5a, b for $\varepsilon \neq 0$. The hydrogen bound-free absorption coefficient which undergoes drastic changes at the absorption edges (see Figure 1a) gives rise to a large change in the magnitudes of p and q as well as their signs, the effect which was predicted by Lamb and Sutherland (1974), for the optically thin case. In all these computations for a slab geometry (Figures 4 and 5) we have neglected the magnetic birefringence. They give an idea of the nature of polarized radiation field at any particular point on the visible disk of the star. It can be noted that p is, in general, very small for the field strength we have chosen.

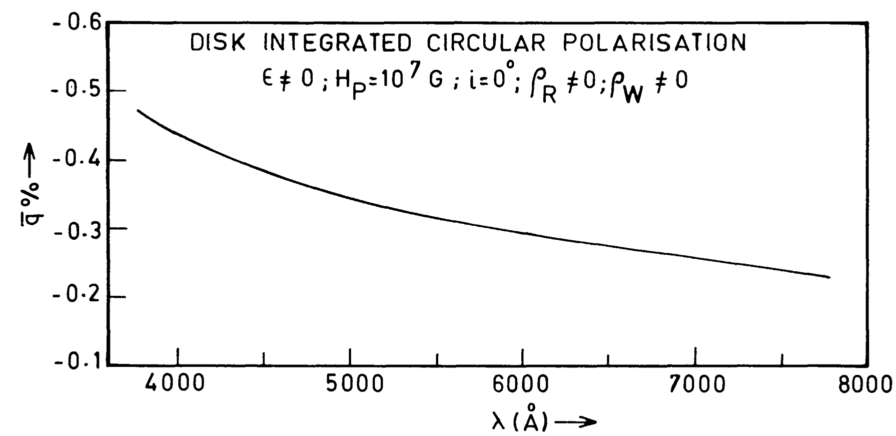

Fig. 6. Wavelength dependence of circular polarization $\bar{q}$ for a dipole field geometry.

In Figure 6 we have plotted the circular polarization spectrum ($\bar{q}v/s\lambda$; $\bar{q} = F_V/F_I$) computed assuming a centred dipole of field strength $H_p = 10^7$ G. The angle i between the dipole axis and the line-of-sight is taken as zero. We have used 8 latitudes and 8 longitudes. The field strengths and orientations are calculated at all the grid points. The transfer equations (1)–(4) are solved at all these grid points, and then rotated properly using Equation (8) to refer the solution to a fixed frame of reference. The solution is then integrated over the disk. The linear polarization $\bar{p} = 0$ because of the symmetry ($i = 0$). The magneto-optical parameters are included, but they do not have significant effect on the values of $\bar{q}$ because of low electron density of the atmosphere. The circular polarization $\bar{q}$ is overestimated because of the lower-order angular quadrature used for averaging over the disk. We conclude that the thermal magneto-absorption model produces expected wavelength dependence of the circular polarization in the atmosphere of a white dwarf. Linear polarization is a very small quantity for weaker fields and more accurate surface averaging is necessary to calculate it correctly. Such calculations are in progress.

Acknowledgements

One of us (A.P.) would like to thank Dr R. Wehrse for several discussions on this topic.

References

Angel, J. R. P.: 1978, *Ann. Rev. Astron. Astrophys.* **16**, 487.
Angel, J. R. P. and Landstreet, J. D.: 1974, *Astrophys. J.* **191**, 457.
Grant, I. P. and Hunt, G. E.: 1968, *Monthly Notices Roy. Astron. Soc.* **141**, 27.
Grant, I. P. and Hunt, G. E.: 1969a, *Proc. Roy. Soc.* **A313**, 183.
Grant, I. P. and Hunt, G. E.: 1969b, *Proc. Roy. Soc.* **A313**, 199.
Gneding, Yu. N. and Pavlov, G. G.: 1974, *Soviet Phys. JETP* **38**, 903.
Kemp, J. C.: 1977, *Astrophys. J.* **167**, 213, 794.
Kuruz, R. L.: 1970, SAO Special Report, No. 309.
Lamb, F. K. and Sutherland, P. G.: 1974, in C. J. Hansen (ed.), 'Physics of Dense Matter', *IAU Symp.* **53**, 265.
Landstreet, J. D. and Angel, J. R. P.: 1975, *Astrophys. J.* **196**, 819.
Liebert, J., Angel, J. R. P., and Landstreet, J. D.: 1975, *Astrophys. J.* **202**, L139.
Martin, B. and Wickramasinghe, D. T.: 1978, *Monthly Notices Roy. Astron. Soc.* **183**, 533.
Martin, B. and Wickramasinghe, D. T.: 1979a, *Monthly Notices Roy. Astron. Soc.* **189**, 69.
Martin, B. and Wickramasinghe, D. T.: 1979b, *Monthly Notices Roy. Astron. Soc.* **189**, 883.
Martin, B. and Wickramasinghe, D. T.: 1981, *Monthly Notices Roy. Astron. Soc.* **196**, 23.
Martin, B. and Wickramasinghe, D. T.: 1982, *Monthly Notices Roy. Astron. Soc.* **200**, 993.
Peraiah, A. and Grant, I. P.: 1973, *J. Inst. Math. Appl.* **12**, 75.
Shipman, H. L.: 1971, *Astrophys. J.* **167**, 165.
Stenflo, J. O.: 1971, in R. Howard (ed.), 'Solar Magnetic Fields', *IAU Symp.* **43**, 101.
Unno, W.: 1956, *Publ. Astron. Soc. Japan* **8**, 108.
Wehrse, R.: 1976, *Astron. Astrophys. Suppl.* **24**, 95.